

## ORIGINAL RESEARCH

# Parched pines: a quantitative comparison of two multi-year droughts and associated mass mortalities of bishop pine (*Pinus muricata*) on Santa Cruz Island, California

Annalise Taylor<sup>1</sup> , Tanushree Biswas<sup>2</sup>, John M. Randall<sup>2</sup>, Kirk Klausmeyer<sup>2</sup> & Brian Cohen<sup>2</sup><sup>1</sup>UC Berkeley Department of Environmental Sciences, Policy, and Management, 130 Mulford Hall #3114, Berkeley California, 94720<sup>2</sup>The Nature Conservancy California Chapter, San Francisco California, 94105

## Keywords

Drought monitoring, Google Earth Engine, Landsat, vegetation index, vegetation mortality

## Correspondence

Annalise Taylor, UC Berkeley Department of Environmental Sciences, Policy, and Management, 130 Mulford Hall #3114, Berkeley, CA 94720. Tel: +1 650 644 9915; Fax: +1 510 643 5438; E-mail: annalise.r.taylor@gmail.com

Editor: Kate He

Associate Editor: Anna Cord

Received: 14 April 2019; Revised: 27 May 2019; Accepted: 21 June 2019

doi: 10.1002/rse2.123

## Abstract

Extreme weather events such as droughts are expected to increase in severity and frequency as the climate changes; it is imperative that land managers be able to monitor associated changes in vegetation health efficiently and across large scales in order to mitigate or prepare for these events. This need motivated deeper study of the die-off of bishop pine (*Pinus muricata*) on California's Santa Cruz Island during the 2012–2016 drought. These pines play a keystone role within the island's ecosystem and have experienced two severe droughts and associated mass die-offs in the past 40 years. In an effort to compare these events, we used meteorological data to track changes in drought severity from 1985 to 2018 coupled with novel methods for forest monitoring to reveal dynamics not detectable by shorter-duration studies. Leveraging 34 years of 30 m resolution Landsat imagery, we compared vegetation mortality between the two most severe droughts of that time period: 1987–1991 and 2012–2016. We used the slope of decline in the annual median value of three different Vegetation Indices (VIs; NBR, NDMI and NDVI) to compare mortality between the two drought events and to reveal spatial patterns of mortality within the bishop pine forests. Our results indicated that the 2012–2016 drought was the island's harshest in over a century and that it resulted in greater and more widespread mortality of vegetation within bishop pine stands than the 1987–1991 drought. The average VI decline was significantly greater during the 2012–2016 drought than the 1987–1991 drought by a factor of 1.89, 2.09 and 1.84 for NBR, NDMI and NDVI, respectively. Our results aligned with projections of increasing drought severity and associated tree mortality across the region. The temporal monitoring methods developed here can be adapted to study similar landscape scale changes over multiple decades in other forest ecosystems facing similar threats.

## Introduction

Forest die-offs have been documented globally during and shortly after periods of severe drought, as the physical stresses and insect outbreaks associated with drought events can result in the deaths of large numbers of trees (Allen et al. 2010; Choat et al. 2012). Droughts and associated diebacks of trees are expected to increase in frequency and intensity in western North America as the region's climate changes, and current drought impacts may provide valuable insights into the potential survival

and structure of forests in the future (Seager et al. 2007; Allen et al. 2010; Woodhouse et al. 2010; Carnicer et al. 2011). From 2012 to 2015, California was affected by one of the most severe droughts recorded since reliable record-keeping began in the mid-1800s (Robeson 2015). Although the northern part of the state was relieved by heavy rainfall in the winter and early spring of 2016, the drought extended through 2016 in Southern California and did not break there until the winter of 2017. By 2016, the US Forest Service reported that 102 million trees had died across the state, with the greatest losses

located in the central and southern Sierra Nevada (Allen et al. 2010; Stevens 2016).

Concern about the die-off of native pine stands on California's Santa Cruz Island deepened as this drought wore on (Kim 2015; Carlson 2016). As early as the summer of 2014, island managers and visiting researchers reported that bishop pines (*Pinus muricata*) were dead and dying in large numbers (Knapp et al. 2015; Taylor 2016). Bishop pine is the only native conifer on the island and is crucial to the survival of some of the island's other native species, including the only island-endemic bird species in the continental United States and Canada, the Island Scrub-Jay (*Aphelocoma insularis*) (Morrison et al. 2011; Langin et al. 2015; Pesendorfer et al. 2017).

Santa Cruz Island is the largest and most biodiverse of the eight California Channel Islands (Schoenherr et al. 2003). It has a mediterranean climate with dry summers and rainless periods often lasting six months or more. During these rainless periods, coastal low clouds and fog (CLCF) often cover parts of the island. The pine's needles capture droplets from the CLCF which condense and drip to the soil beneath; as summer precipitation is highly limited on the island, the cloud- and fog-harvesting pines play a critical role by capturing moisture and delivering it to the soil (Brumbaugh 1980; Walter and Taha 1999; Carbone et al. 2013). The bishop pine itself is partially dependent on the moisture it harvests from CLCF – and the reduction in evapotranspiration that occurs beneath CLCF – to survive the dry season and other periods of drought stress (Williams et al. 2008; Fischer et al. 2009, 2016).

Santa Cruz Island's bishop pine forests were known to have experienced an extensive die-off associated with an earlier drought from 1987 to 1991 (Wehtje 1994; Walter and Taha 1999). This die-back had been noteworthy because the island's vegetation, including the bishop pine stands, had been recovering rapidly from overgrazing by feral sheep for several years prior to the onset of the 1987–1991 drought following the removal of sheep from most of the island by the mid-1980s (Wehtje 1994; Junak 1995). In addition, two other severe droughts accompanied by bishop pine mass mortality events have been reported on Santa Cruz Island, one in the late 1940s and another in the mid-1970s (Fischer et al. 2009). Baguskas et al. (2014) studied bishop pine mortality within one stand on Santa Cruz Island during a relatively short drought from 2007 to 2009 (Baguskas et al. 2014). That study showed that the highest densities of dead bishop pine trees occurred in the drier and more inland margins of the stands and that greatest survivorship occurred among larger trees (8 to 10 m tall) at moderate elevations which were more commonly enveloped within a layer of CLCF (Baguskas et al. 2014).

Given the bishop pine's globally limited distribution and vulnerable ranking by the IUCN, its mass mortality on Santa Cruz Island during the recent drought raised concerns and calls for quantitative investigation into its extent and severity (Farjon 2013). As is true for many drought impact studies, past research on the island's pines had been temporally limited. However, in order to manage these ecosystems within the context of changing drought conditions on the island, researchers and conservation managers needed to compare the recent drought to past droughts with regard to both severity and bishop pine mortality. Fortunately, the continuity of Landsat's multispectral imaging satellites enables powerful comparisons across long time periods that are not possible with spatially and temporally limited field data (Robinson et al. 2017). Landsat's imaging satellites have operated continuously for 45 years – longer than any other remote sensing imagery collection program – and therefore offer a unique view of changes on the earth's surface over time (Irons et al. 2012). Landsat time series analyses represent an exciting expansion of the field of remote sensing in ecology and specifically long-term ecosystem monitoring (Pasquarella et al. 2016). In particular, free, analysis-ready Landsat data coupled with the advances in image processing and computational capacity available through Google Earth Engine provides scientists with robust tools to monitor ecosystems in real time.

Because the 30 m resolution Landsat imagery is moderately coarse in relation to the bishop pine's canopy, we focused our analysis on bishop pine-dominated communities (BPDCs) – as defined by the best available vegetation dataset on the island – to reduce the influence of other species on the analysis (Cohen et al. 2009). Using Google Earth Engine to analyze 34 years of the Landsat archive on Santa Cruz Island, our three objectives were to: (1) determine the extent and severity of vegetation mortality within BPDCs during the 2012–2016 drought; (2) compare results with mortality associated with the 1987–1991 drought, and (3) target potential refugia from drought (Morelli et al. 2016; McLaughlin et al. 2017). Our methods compared patterns of forest mortality over decades and between two major drought events, and represent efficient means for monitoring this keystone species into the future.

## Materials and Methods

### Study area

Santa Cruz Island (34.0036° N, 119.7264° W) is the largest of the eight California Channel Islands at approximately 250 km<sup>2</sup> (Fig. 1) (Wehtje 1994). Located approximately 40 km south of Santa Barbara, 76% of the island is owned and managed by The Nature Conservancy



**Figure 1.** Global distribution of bishop pine (*Pinus muricata*) as mapped by the United States Geological Survey (Little 1999). Bishop pines (shown in blue) are found in scattered stands from Humboldt County, California in the north to a site near San Vicente, Baja California and Isla Cedros, Baja California, in the south. Santa Cruz Island ( $34.0036^{\circ}$  N,  $119.7264^{\circ}$  W) is located approximately 40 km south of Santa Barbara, California.

as a nature preserve, and the remaining 24% is owned and managed by the U.S. National Park Service as part of Channel Islands National Park. The island's mediterranean climate is marked by relatively warm, dry summers and cooler, wetter winters. Differences in topography and distance from the ocean on the island create variations in temperature, rainfall and CLCF cover at different sites (Boyle and Laughrin 2000; Fischer and Still 2007; Baguskas et al. 2014). Weather data gathered near the main ranch on the island reveal that roughly 80% of the precipitation falls between November and March (Fig. 2) (Junak 1995). CLCF is most persistent over the four northern Channel Islands from May to September (Rastogi et al. 2016).

The island is home to scattered individuals and dense stands of bishop pine which together represent a large

fraction (almost 10%) of the species' global distribution (Fig. 1) (Little 1999). Figure 2 shows three of the bishop pine stands on Santa Cruz Island. The stands vary in size, density, climate and soil type, and were delineated in 2007 as part of an island-wide vegetation mapping effort that consisted of stereoscopic aerial photo interpretation combined with ground surveys and field checks, with a minimum mapping unit of one-half hectare (Cohen et al. 2009). Due to cost, bishop pine communities were mapped to the alliance or vegetation community level rather than species level; therefore, we restricted our study to regions on the island classified as bishop pine-dominated alliances, in which bishop pine cover values were at least 40% (Cohen et al. 2009). We refer to these regions as bishop pine-dominated communities (BPDCs), which cover 171.8 ha of the island. The restriction of our study area to BPDCs aimed to reduce interference from other vegetation types in the Landsat imagery we used. We further restricted our analysis by using a 15 m interior buffer to ensure that Landsat pixels included in the analysis fell completely within the BPDCs. As a result, our study area totaled 105.8 ha and encompassed the densest patches of bishop pine habitat on the island (Fig. 2).

### Drought comparison

To determine the length and severity of past and current droughts on the island, we calculated the spatial average of the Palmer Drought Severity Index (PDSI) at 4 km spatial resolution and 10 day temporal resolution within the study area. The PDSI is a climatic index developed to estimate the length and severity of long-term drought using a computation involving soil moisture, potential evapotranspiration (PET) and precipitation (Alley 1984). PET and precipitation were derived from Abatzoglou's gridded meteorological dataset (Abatzoglou 2013; Abatzoglou et al. 2014). Abatzoglou calculated PET using the Penman-Montieth equation for a reference grass surface and used the STATSGO soil database to derive the water-holding capacity of the soil at any given point (Huang et al. 2010). PDSI values generally range between  $-4$  and  $4$ , where negative values indicate increasing severity of drought. As the PDSI is defined, values below  $-2.0$  indicate moderate drought, values below  $-3.0$  indicate severe drought, and values below  $-4.0$  indicate extreme drought (Alley 1984).

Given the coarse resolution of PDSI data, precipitation records from a weather station located near Santa Cruz Island's main ranch (152 m elevation) were used to supplement these data to confirm the durations of the droughts on a local scale (Fig. 3) (Boyle and Laughrin 2000; Laughrin 2017).

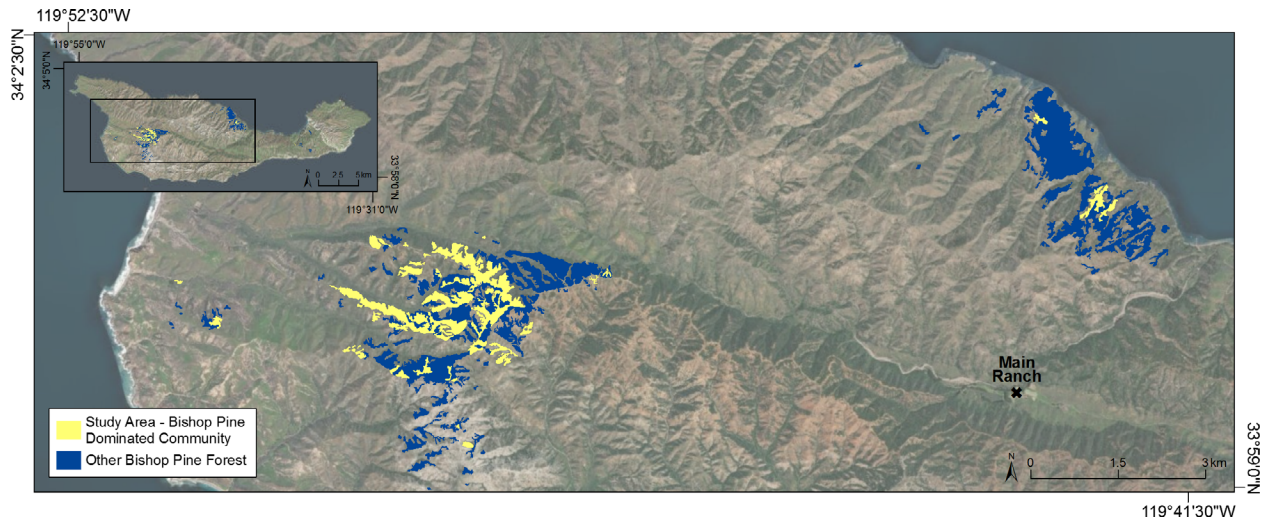


**Figure 2.** The distribution of bishop pine on Santa Cruz Island as mapped by Cohen et al. (2009). The study area consisted of a subset of the distribution for which bishop pine represented the dominant vegetation type (BPDCs, shown in yellow). Areas for which bishop pine did not represent the dominant vegetation type (shown in blue) were excluded from the analysis to improve accuracy. A label shows the location of the main ranch on the island where weather data were collected. The inset map shows the location of the study area on Santa Cruz Island.

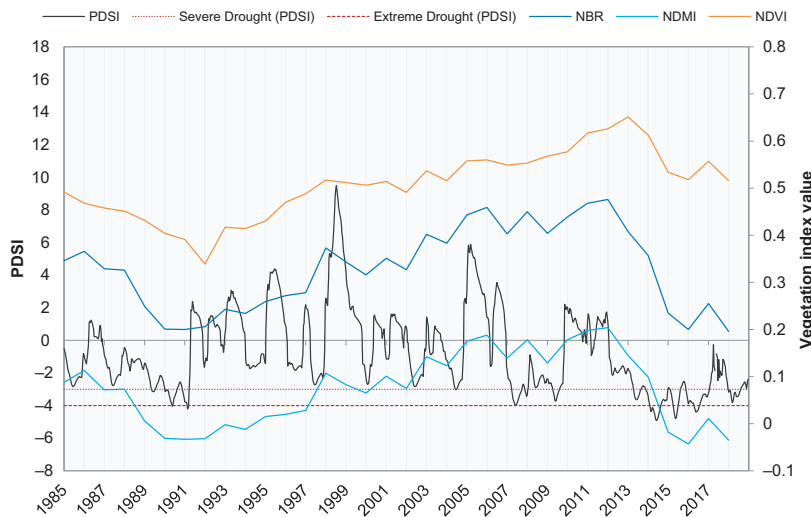


**Figure 3.** Annual median values of three vegetation indices (NBR, NDMI, and NDVI) overlaid with PDSI values within the study area, from 1985 to 2018. Dotted red lines indicate PDSI thresholds for severe (-3.0) and extreme (-4.0) drought conditions, as defined by PDSI.

**Satellite imagery**

Our study used Google Earth Engine, a web-based application programming interface (API) that enables rapid analysis of large spatial datasets (Gorelick et al. 2017). Having defined the spatial extent of our study area using ArcMap 10.6, we ingested the shapefile into Google Earth Engine and conducted all of our drought and imagery analyses using datasets available within the API (Environmental Systems Research Institute 2018).

Moderate resolution (30 m) surface reflectance imagery from Landsat 5 (Enhanced Thematic Mapper), Landsat 7 (Enhanced Thematic Mapper Plus) and Landsat 8 (Operational Land Imager) sensors were used to derive

vegetation indices across the study area from 1985 to 2018. The Landsat archive on Santa Cruz Island during the study period totaled 802 images which are captured roughly every 16 days, as sourced from three separate satellite missions (Irons et al. 2012). CFMask, an automated cloud-masking algorithm incorporated into the Landsat surface reflectance imagery available in Google Earth Engine, was used to filter and remove pixels containing clouds, cloud shadows, and other errant pixels from the selected images (Foga et al. 2017).

**Vegetation indices**

Multispectral satellites such as Landsat capture electromagnetic radiation within spectral bands that span visible

and infrared wavelengths. These bands can be transformed to reveal attributes about vegetation on the earth's surface, such as its canopy structure, chlorophyll content, and water content (Deshayes et al. 2006; Jones and Vaughan 2010). Living vegetation absorbs radiation in portions of the visible spectrum and reflects in the near-infrared (NIR), whereas radiation in the shortwave-infrared (SWIR) is absorbed by water present in the leaves (Jones and Vaughan 2010). Therefore, NIR and red wavelengths are sensitive to variations in greenness, and SWIR wavelengths are sensitive to water stress during periods of drought (Deshayes et al. 2006). Numerous spectral vegetation indices have been used to study vegetation health, drought impacts on vegetation, and deforestation, many of which utilize red, NIR, and/or SWIR wavelengths. In order to study the effects of drought within BPDCs, we used three vegetation indices: Normalized Difference Vegetation Index (NDVI) (Maselli 2004; Weiss et al. 2004; Volcani et al. 2005; Lloret et al. 2007), Normalized Difference Moisture Index (NDMI) (Goodwin et al. 2008; Meddens et al. 2013; Walter and Platt 2013), and Normalized Burn Ratio (NBR) (Wang et al. 2008). We used all three of these indices to investigate their differing sensitivities to bishop pine mortality (Table 1).

These three VIs were calculated for each pixel of each image (802 images in total) and appended to the images as additional bands. We then calculated the annual median value from the cloud- and shadow-free pixels for each spectral band and VI over the entire 34-year period to create a cloud-and shadow-free annual median composite image across the study area. Thus the stack of 802 images was reduced to 34 images where each pixel contained the annual median value of each VI (as calculated from a varying number of individual cloud- and shadow-free pixels available in a given year at that pixel's location). These annual median composites reduce the effects of temporal variability in the data, as well as any errant pixel values not filtered out by the CFMask algorithm.

**Table 1.** Spectral indices calculated from Landsat surface reflectance data: Normalized Burn Ratio (NBR), Normalized Difference Moisture Index (NDMI), and Normalized Difference Vegetation Index (NDVI)

Spectral Index	Equation	Source
NBR	$NBR = (NIR - SWIR) / (NIR + SWIR2)$	Key and Benson (2005)
NDMI	$NDMI = (NIR - SWIR) / (NIR + SWIR1)$	Wilson and Sader (2002)
NDVI	$NDVI = (NIR - red) / (NIR + red)$	Rouse (1974)

## Temporal analysis and comparison

We computed the spatial averages of the cloud-free annual median composite pixel values of NBR, NDMI, and NDVI within the study area and compared them to the spatial average of the PDSI across the same time period to explore the relationship between forest health and the drought cycle.

To compare the intensity of mortality within the BPDCs between the two droughts (1987–1991 and 2012–2016), we used the simple linear regression of the annual median values to calculate the ratio of change between the two drought periods for each VI. One-way ANOVA was used to test if the differences in slopes between the 2012–2016 and 1987–1991 droughts were significant. A ratio of the slope of each VI between the two drought periods compared the severity of BPDC mortality between the two drought periods.

## Spatial analysis and comparison

We ran a pixel-by-pixel analysis across the study area to compare spatial patterns and extent of vegetation mortality within BPDCs. We mapped the average annual change in each VI during both the 1987–1991 and 2012–2016 droughts using identical visualization parameters to allow direct comparison between VIs and time periods. We then ran a pixel-level analysis of the regression of the slope and masked out those pixels for which the  $R^2$  of the slope was  $<0.60$ .

Next, we calculated the difference in average annual changes in each VI between the 2012–2016 and 1987–1991 droughts by subtracting the former from the latter on a pixel-by-pixel basis. Thus, a difference close to 0.0 indicated little difference in the rate of mortality between the two droughts at that pixel, a positive difference indicated that the rate of mortality was greater in the 2012–2016 drought than in the 1987–1991 drought, and a negative difference indicated the opposite. Identical visualization parameters were again used to allow spatial comparison of variation in mortality across each vegetation index.

## Drought refugia

We categorized potential drought refugia as those pixels for which the rate of change in a VI was greater than or equal to 0.0 during both droughts. This was based on an assumption that an area with no average annual change or a positive average annual change likely indicates minimal BPDC mortality. This conservative threshold allowed us to identify sites whose physical characteristics (curvature of the slope, aspect, CLCF frequency, etc.) may allow them to retain enough soil moisture even during

prolonged droughts to allow some portion of the adult bishop pines to survive.

### Validation of methods

To validate our results, we ran a supervised classification of two high resolution images from the U.S. Department of Agriculture's National Agriculture Imagery Program (NAIP), captured on 5 May 2012 (1.0 m resolution) and 25 June 2016 (0.6 m resolution). These images contained four spectral bands: blue, green, red, and near-infrared wavelengths. Individual pines were clearly visible at this resolution and a false color visualization increased the contrast between living and dead vegetation. In each image, an observer visually classified training points within the BPDCs into three categories: dead vegetation, living vegetation and open ground ( $n_{2012} = 435$ ;  $n_{2016} = 684$ ). For each time period, these points were used to train a Random Forest classifier with 1000 decision trees to classify the NAIP pixels into dead vegetation, living vegetation or open ground (Appendix S1) (Liaw and Wiener 2002). The training accuracy was 100.0% for the 2012 classification and 99.71% for the 2016 classification. A separate observer then identified 100 validation points with an equal distribution among the three cover classes for each image ( $n_{2012} = 100$ ;  $n_{2016} = 100$ ). The validation accuracy was 89.0% for the 2012 classification and 96.0% for the 2016 classification.

The high accuracy of these classified NAIP images allowed us to quantify and compare vegetation mortality between 2012 and 2016 in order to validate the trends we observed from the Landsat time series analysis. To do this, we extracted Landsat pixels that were completely contained within the BPDCs ( $n = 1859$ ) and calculated the percentage of the three vegetation classes within each pixel, as classified in the NAIP image. In addition, we evaluated the correlation between the NAIP-derived vegetation class (dead vegetation, living vegetation and open ground) and the Landsat-derived annual median VI values. A Random Forest regression (Liaw and Wiener 2002) was used to predict the percentage of living vegetation within each Landsat pixel as a function of the nine Landsat bands and indices.

## Results

### Drought comparison

During the 34-year study period from 1985 to 2018, the PDSI indicated that the study area experienced two severe droughts (1987–1991 and 2007–2009) and one extreme drought (2012–2016) (Fig. 3). Although the three-year 2007–2009 drought was characterized as severe for 12 months within the study area, heavy rain in early 2008 effectively split this drought into two shorter, roughly year-

long droughts. Our methods aim to capture inter-annual variations in vegetation mortality and therefore are not suited to study changes in forest health within a given year. Rather, this study analyzed only the two lengthier 5-year droughts (1987–1991 and 2012–2016) in more depth. Conditions were severe for 21.1% (14 months) of the 1987–1991 drought and extreme for 2.2% of the period (1.3 months). During the 2012–2016 drought, conditions were severe for over twice as long (41.7% of the period; 36.3 months) and extreme for nearly 10 times as long (21.1% of the period; 12.6 months) (Fig. 3).

### Temporal analysis and comparison

During both drought periods (1987–1991 and 2012–2016), we observed a decline in all three VIs within the study area (Fig. 3). The trends of the three VIs appeared to follow the drought cycle present on the island. The decline in all three VIs at the onset of the 1987–1991 drought followed a sharp decline in PDSI, and the VIs did not begin to increase from their 1987–1991 lows until approximately 12 to 18 months after an abrupt increase in the PDSI due to the 'Miracle March' rains of March 1991 (Boyle and Laughrin 2000). The decline in each VI at the onset of the 2012–2016 drought lagged slightly behind an abrupt drop in PDSI. As the PDSI had not yet consistently trended upwards by the end of 2018 (except briefly due to winter storms in late 2016 and early 2017), Santa Cruz Island remained in a state of drought.

In both prolonged drought periods (1987–1991 and 2012–2016), all VIs declined consistently, indicating increasing mortality within the study area (Figs. 3 and 4). For both droughts, the average annual decline in NDMI was the largest, followed by NBR and then NDVI (Fig. 4 and Table 2).

The slope of decline was between 1.84 and 2.09 times greater during the 2012–2016 drought than in the 1987–1991 drought for all three VIs (Table 2). The slopes of NBR and NDMI were significantly more negative during the recent drought than the one previous, as determined using one-way ANOVA (NBR:  $F = 11.69$ ,  $P = 0.014$ ; NDMI:  $F = 12.97$ ,  $P = 0.011$ ; NDVI:  $F = 2.41$ ,  $P = 0.17$ ). Steeper and more negative slopes indicated greater average annual decline during the 2012–2016 drought, which aligns with our hypothesis that the intensity of drought and associated BPDC mortality was greater in 2012–2016 than in 1987–1991.

### Spatial analysis and comparison

Our spatial investigation of vegetation mortality revealed widespread declines in all three VIs and across both droughts, although the extent and intensity varied

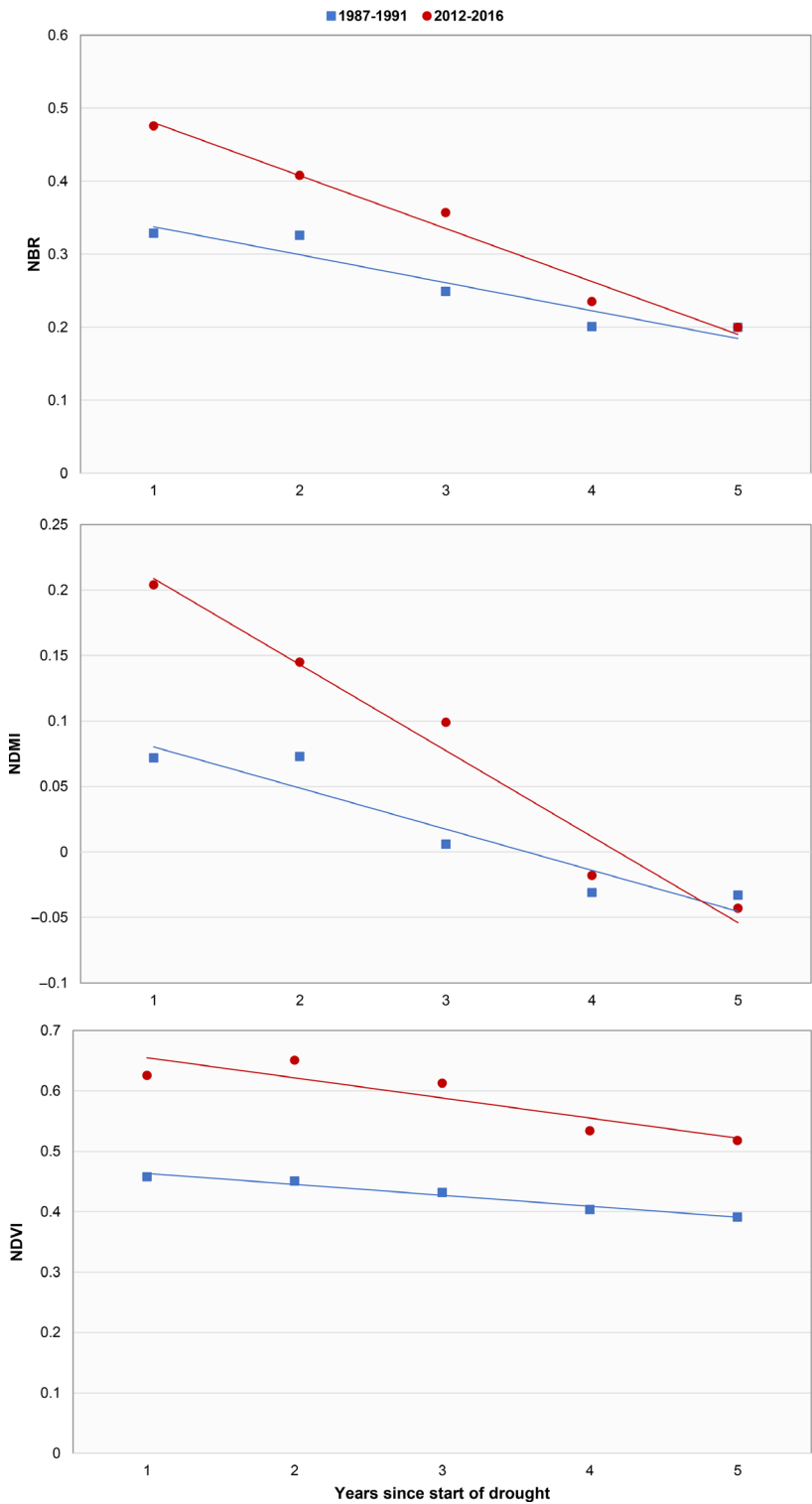


**Figure 4.** Median values of NBR, NDMI and NDVI within the study area during the 1987–1991 and 2012–2016 droughts. Colored lines indicate the linear regression of each drought trend across all three VIs.

between the two periods (Fig. 5). While the 1987–1991 VI declines are concentrated in the northwestern region of the study area, the 2012–2016 VI declines cover most of the study area (Fig. 5).

The slope of the VI declines during the 2012–2016 drought was greater than that of the 1987–1991 drought for 88.6%, 92.1% and 75.3% of the study area for NBR, NDMI and NDVI, respectively (Fig. 6). NBR and NDMI

**Table 2.** Average annual decline in all three VIs during both drought periods and the ratio of the average annual decline between the 1987–1991 drought and the 2012–2016 drought for each VI. Asterisks indicate a significant difference ( $P < 0.05$ ) between the two drought periods

	NBR*	NDMI*	NDVI
1987–1991	−0.0383	−0.0314	−0.0181
2012–2016	−0.0725	−0.0657	−0.0333
Ratio	1.893	2.092	1.840

indicate that BPDC mortality during the 2012–2016 drought was much more severe than that of the 1987–1991 drought across almost all of the study area (Fig. 6). NDVI also indicates that BPDC mortality during the 2012–2016 drought was more severe across most of the study area, but it reveals some regions along the northern edge of the study area that may have experienced sharper declines during the 1987–1991 drought (Fig. 6).

We categorized portions of the study area where the average annual change in VI values was equal to or

$>0.0$  during either drought as potential drought refugia, however, none of these pixels had a slope with an  $R^2$  value equal to or  $>0.60$  and are therefore not shown in Fig. 5. The extent of these potential drought refugia ranged between 2.14% and 8.21% of all BPDCs during the 1987–1991 drought and between only 0.71% to 1.43% during the 2012–2016 drought (Table 3). As compared to the 1987–1991 drought, the percentage of the study area classified as potential drought refugia decreased by  $-1.43\%$ ,  $-4.64\%$  and  $-6.79\%$  for NBR, NDMI and NDVI respectively during the 2012–2016 drought (Table 3).

### Validation of methods

Our validation showed that the mean percentage of the grid cells classified as dead vegetation in the NAIP imagery increased significantly between 2012 and 2016 ( $t = -43.76$ ,  $df = 2999.3$ ,  $P < 0.001$ ), while the mean percentage of the grid cells classified as living vegetation decreased significantly ( $t = 38.39$ ,  $df = 3576.5$ ,  $P < 0.001$ )

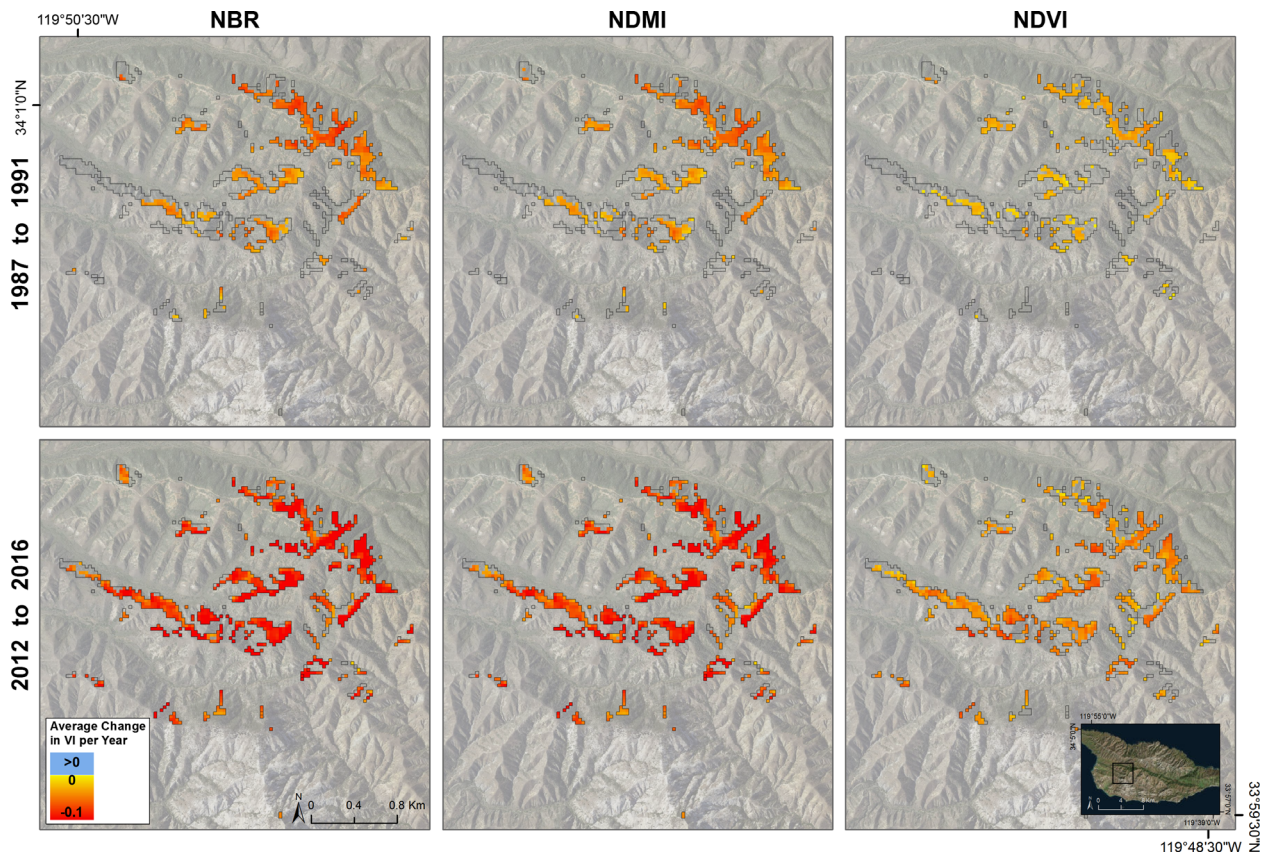


**Figure 5.** Spatial variation in the average annual change in the median values of NBR, NDMI and NDVI within the western portion of the study area during the 1987–1991 and 2012–2016 droughts. Pixels for which the  $R^2$  value of the regression of the slope was  $<0.60$  are not shown. Inset map shows the location of the western portion of the study area within the entire study area.



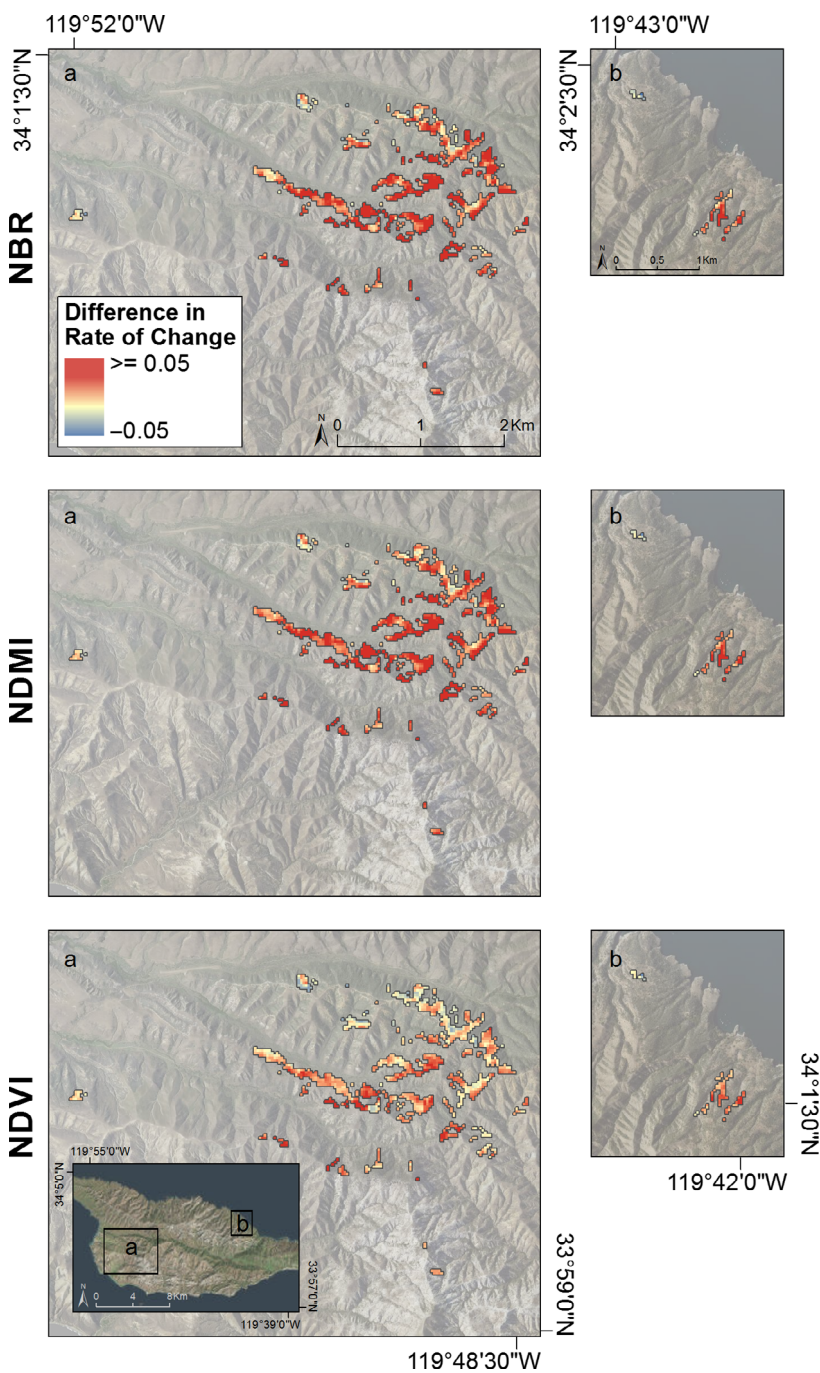


**Figure 6.** Difference in the average annual change in the median values of NBR, NDMI and NDVI over the study area between the 1987–1991 and 2012–2016 drought events. A difference of zero in the rate of change indicates little difference in the rate of mortality between the two droughts (shown in yellow), a positive difference indicates that the intensity of mortality was greater in the 2012–2016 drought (shown in red) and a negative difference indicates the opposite (shown in blue). Inset map shows the location of the two detailed zoom maps on Santa Cruz Island.

**Table 3.** Total area and percentage of study area with potential to act as drought refugia during the 1987–1991 drought as compared to the 2012–2016 drought. Potential drought refugia were defined as pixels within the study area for which the rate of change of a vegetation index was greater than or equal to 0.0

	1987–1991 (hectares)	2012–2016 (hectares)	1987–1991 (% of study area)	2012–2016 (% of study area)	Percent Change
NBR	2.023	0.674	2.14%	0.71%	–1.43%
NDMI	5.141	0.758	5.45%	0.80%	–4.64%
NDVI	7.753	1.348	8.21%	1.43%	–6.79%

(Appendix S2). The mean per cent cover of open ground within the pixels differed between the two periods but remained minimal ( $t = -7.71$ ,  $df = 3575.6$ ,  $P < 0.001$ ; 95% Confidence Intervals (CI)  $CI_{2012}$ : 7.52%, 8.41%;  $CI_{2016}$ : 10.19%, 11.28%). These results support our hypothesis that a decline in living vegetation and increase in dead vegetation contributed to the decline in VIs as derived from Landsat imagery within the BPDCs, and at minimum prove that the declining VI trends between 2012 and 2016 coincide with an increase in dead vegetation within the BPDCs.

The overall relationship between percentage of living vegetation quantified from NAIP imagery and vegetation health predicted from Landsat indices had an  $R^2$  value of 0.554% ( $MSR = 231.50$ ). In predicting living vegetation, NBR, NDMI and NDVI were ranked 2nd, 3rd and 4th in the variable importance plot (Appendix S3).

## Discussion

### Drought comparison

Our analysis of drought conditions indicated that the 2012–2016 drought was harsher than the 1987–1991 drought, and that BPDC mortality on the island was greater and more widespread during and immediately following the 2012–2016 drought (Fig. 3). Given that Fischer et al. (2009) found that the 1987–1991 drought was the worst of the 20th Century on the island, our findings indicate that the 2012–2016 drought was the harshest in at least 115 years (Fischer et al. 2009). The greater drought severity and mortality of BPDCs during the 2012–2016 drought is in line with projections for increasing severity of both droughts and tree mortality across southwestern North America as the climate continues to warm (Seager et al. 2007; Allen et al. 2010; Woodhouse et al. 2010; Carnicer et al. 2011). As the 2012–2016 drought event is the harshest in over a century, post-drought recovery of the bishop pine forest merits further study. In addition to this historical comparison, the methods explored here demonstrate a novel approach to monitor drought impacts across large spatial scales and at frequent temporal intervals.

The results of our VI analyses indicate that the die-off of BPDCs was more severe during the 2012–2016 drought than during the 1987–1991 drought (Table 2, Fig. 4). Consistent decline in all three VIs and significant increases in the magnitude of the decline support our hypothesis that periods of harsher drought will result in greater cumulative mortality of BPDCs and that this effect is quantifiable with Landsat imagery. Further, we restricted our study area to the densest bishop pine stands which may represent the best pine habitat on the island,

suggesting that our results are conservative and that bishop pine mortalities may be even greater elsewhere on the island.

Our spatial analyses reveal important differences between and advantages of each of the VIs used. NDMI and NBR utilize different portions of the SWIR range: NDMI uses SWIR1 (sensitive to moisture content in the leaves), while NBR uses SWIR2 (higher sensitivity to dead woody vegetation) (Wilson and Sader 2002; Key and Benson 2005; Assal et al. 2016). Our results show the steepest decline in the slope of NDMI as compared to the other VIs during the 2012–2016 drought, which could mean that NDMI was most sensitive to this mortality event (Fig. 4). While NBR is primarily used to identify burned areas, we found NBR to be effective in capturing the impact of drought given its sensitivity to standing dead trees (Key and Benson 2005; Wang et al. 2008). While NDVI is a good indicator of healthy vegetation, our study joins others in suggesting that a combination of VIs can provide increased insight into the progression of drought-impacted mortality events within pine-dominated forests (Cohen et al. 2010, 2017; Barrett et al. 2016).

### Drought refugia

We defined potential drought refugia as areas for which the average annual change in VI values was greater than or equal to 0.0 during either drought. We speculated that areas with little to no decline in VI value experienced little or no loss of living vegetation cover. Our conservative threshold revealed that a very small percentage of the study area served as potential drought refugia during the 2012–2016 drought across all three VIs (Table 3). Furthermore, all of the areas classified as potential drought refugia had  $R^2$  values of  $<0.60$ , which indicates that there were no sites which consistently had no change in VI or a positive trend in VI (Fig. 5). This is likely due in part to two possibilities, both of which merit further study: (1) this drought-impacted BPDCs to such an extent that even areas that served as refugia during previous droughts experienced mortality or (2) the criteria we used do not accurately capture drought refugia. Our data indicated that the VI declines were weaker along the western reaches of the BPDCs relative to the rest of the study area, but further research will be needed to determine if these locations potentially serve as drought refugia for bishop pine. Methods to define drought refugia using remote sensing analyses such as these represent an important area of future study (Morelli et al. 2016; McLaughlin et al. 2017).

While our study focused primarily on precipitation as it related to forest mortality, future work might incorporate measures of cloud cover as it has been shown to impact bishop pine survival during shorter periods of

drought (Baguskas et al. 2016; Fischer et al. 2016). CLCF contributes both fog drip and shading which serve to reduce water deficits for bishop pines during the summer months on the island (Carbone et al. 2013). However, we do not have reliable observations or other measures of CLCF and cannot be sure that the frequency and extent of CLCF decreased in tandem with rainfall during the drought periods (Baguskas et al. 2016). Our observations during the 2012–2016 drought revealed that saplings and seedlings could often be found in apparently healthy condition in the midst of stands where most of the adult trees had died (Taylor 2016). This may be due to the progressive decrease of soil moisture at depths typically accessed by adult trees, while moisture inputs from CLCF to the soil's surface layers may have been sufficient to support saplings (Carbone et al. 2011; Baguskas et al. 2016). Baguskas et al. (2016) found that CLCF had far greater positive effects on bishop pine saplings than on adult trees, which they suggested was due to this depth effect. Therefore, CLCF merits further study as a potentially important factor for coastal forest drought refugia.

### Post-drought regeneration

Our VI trends indicate that BPDCs recovered steadily starting shortly after the end of the 1987–1991 drought until the start of the 2012–2016 drought, albeit with at least two notable downturns associated with shorter droughts in the early 2000s and from 2007 to 2009 (Fig. 3). These results align with similar multitemporal analyses of Landsat imagery that showed that the recovery of forest ecosystems was gradual, often requiring more than 10 years (Cohen et al. 2010; Kennedy, Yang, and Cohen 2010; Verbesselt et al. 2010). We did not observe a plateau in any of the VI trends, which may indicate that the forest had not fully recovered prior to the onset of the 2012–2016 drought. As we continue monitoring this population of bishop pines, closer study of the forest's recovery will inform how to best interpret the observed spectral trends.

Given that the severity and frequency of droughts are expected to increase in western North America, it is possible that the island's bishop pine stands may never fully regenerate (Diffenbaugh et al. 2015; Byer and Jin 2017). The loss of bishop pine from the island would not be unprecedented, as there is evidence that other conifers (*Pseudotsuga menziesii* and *Cupressus goveniana*) were eliminated from the island following climatic warming and drying at the end of the last glacial period (Chaney and Mason 1930; Fergusson and Libby 1963; Anderson et al. 2008). As a relict species highly dependent on CLCF, the bishop pine may serve as a harbinger for other fog-sensitive conifers, such as the Santa Rosa Island

Torrey pine (*Pinus torreyana* var. *insularis*) and the coast redwood on the mainland (*Sequoia sempervirens*) (Johnstone and Dawson 2010).

### Validation

In the absence of robust field data, our validation methods make use of high resolution NAIP imagery for classification of changes in vegetation mortality during the 2012–2016 drought. The supervised classifications were highly accurate for each time period and resulted in an 89–96% accuracy rate when tested on an independent validation dataset. Drastic declines in NAIP-classified living vegetation between 2012 and 2016 validate our assumption that decline in the three Landsat-derived VIs did, in fact, indicate increased mortality within the BPDCs (Appendix S2). However, for a number of reasons this two-image comparison may not be suited for direct comparison with our Landsat time series analysis. Kennedy et al. (2010) warn that change analyses based on two-date change detection methods introduce noise and variation associated with each single time period and may not relate directly to multitemporal analyses (Kennedy et al. 2010). For example, the two images were captured at different times of day, causing variable shadow patterns on the hills, as well as different times of the year, introducing variability from the seasonal phenology of surrounding vegetation. Despite these limitations, we found a fairly strong relationship ( $R^2 = 0.55$ ) between the percentage of living vegetation (as classified with NAIP imagery) and Landsat-derived VIs. A variable importance plot showed that these three VIs were top predictors in the model (Appendix S3). These results underscore our finding that combinations of VIs used together provide a more robust method for monitoring vegetation than when treated individually. Future work might involve continued validation of these methods within relatively controlled environments for which field data are available, such as the work by Verbesselt et al. (2010) to track the slope of NDVI (as derived from MODIS imagery, 250 m spatial resolution) with forest growth and harvesting in a controlled environment (Verbesselt et al. 2010).

Our analysis was somewhat limited by the lack of high resolution spatial vegetation data on Santa Cruz Island. While we were able to study vegetation mortality within bishop pine-dominated communities, we were not able to completely isolate our analysis to bishop pines. Future work will benefit from ongoing vegetation mapping efforts on the island. While NAIP imagery provided us with an indirect method to validate our results, our study emphasizes the continued importance of long-term field monitoring plots in validating trends observed from space.

## Advances in time series analysis

Our study builds upon previous work that has linked temporal trends in VIs to forest disturbance and regrowth and seeks to address many of the limitations and warnings offered by these foundational studies (Cohen et al. 2010; Huang et al. 2010; Kennedy et al. 2010; Vogelmann et al. 2012). Verbesselt et al. (2010) warn that change detection methods employing a limited number of images risk classifying short-term variability as longer-term change; Google Earth Engine enables the rapid analysis of high temporal densities of data, which strengthens the signal to noise ratio and can reveal new insights about ecosystem cycles (Robinson et al. 2018; Cohen et al. 2010; Verbesselt et al. 2010). In the absence of Google Earth Engine, a hyper-temporal analysis such as ours would have required advanced storage and processing capabilities that would have presented a considerable barrier to this research. In addition, many change detection methods are designed to detect deviations or single dramatic changes, and can be poor indicators of the gradual trends that we would expect from longer periods of drought mortality and subsequent forest recovery (Cohen et al. 2010; Kennedy et al. 2010; Verbesselt et al. 2010). In a novel approach to this problem, we calculated pixel-based annual median composites values, which reduced the effects of seasonal and image-specific variability and revealed longer-term trends. Lastly, change detection methods reliant on a threshold are highly sensor- and site-dependent; our methods maintain broad applicability by tracking relative changes in each VI (Kennedy et al. 2010; Verbesselt et al. 2010; Fraser et al. 2011; Vogelmann et al. 2012; Forkel et al. 2013). Ultimately, we found that the processing capacity and speed afforded us by Google Earth Engine addressed key limitations currently present in this field (Palumbo et al. 2017). We hope the increased adoption of this free tool will expand the use of a greater number of images and the analysis of multiple VIs in future remote sensing studies.

## Conclusions

This 34-year analysis shows that the 2012–2016 drought was more extreme and prolonged than that of the harshest drought of the previous century on Santa Cruz Island (1987–1991), and that it resulted in greater and more widespread mortality of vegetation within bishop pine-dominated communities, which are vital to the survival of other rare and endemic species. Our spatial analyses have revealed small areas that may serve as potential drought refugia for bishop pines and associated species, which can be targeted for future study to determine whether and why they might actually serve as refugia from which bishop pine populations can re-expand following future droughts.

Changes in global forest cover have important implications for the study of biodiversity, the atmospheric carbon budget, and climatic changes (Huang et al. 2009; Powers et al. 2017). However, field-based long-term ecological monitoring studies of forests are costly and rare, and analyzing the full Landsat archive previously required months or years due to the associated demands on storage and processing power (Kerr and Ostrovsky 2003; Lindenmayer et al. 2012). Our method analyzes 802 images using multiple VIs in less than a minute and demonstrates the power of Google Earth Engine to generate a decades-long quantitative view of an ecosystem. This landscape-scale analysis can be applied to other conifer species and other extreme climate events to efficiently study and monitor forest health across vast expanses of land, and may ultimately reveal previously undiscovered vegetation dynamics.

## ACKNOWLEDGMENTS

This research, the preliminary fieldwork and the costs of publishing were funded by The Nature Conservancy with funds from Martha Blackwell. This research was made possible with open access to Google Earth Engine and support from Peninsula Open Space Trust. We thank Maggi Kelly and two anonymous reviewers for their helpful suggestions on the manuscript.

## Conflict of Interest

The authors declare no conflict of interest. The founding sponsor had no role in the design of the study; in the collection, analyses or interpretation of data; in the writing of the manuscript and in the decision to publish the results.

## Data Accessibility

This study utilized Landsat, PDSI and NAIP data that are publicly available within the Google Earth Engine platform. Vegetation data from Cohen et al. (2009) (<https://arcgis.com/home/item.html?xml:id=620f1115e07e456b95665d079e8a240d>) and high resolution imagery of Santa Cruz Island from the National Park Service (<https://arcgis.com/home/item.html?xml:id=a354bd042c97402aa0b025045313493f>) are available through ArcGIS Online. Please contact [annalise.r.taylor@gmail.com](mailto:annalise.r.taylor@gmail.com) to request access to the scripted analysis in Google Earth Engine.

## References

- Abatzoglou, J. T. 2013. Development of gridded surface meteorological data for ecological applications and modelling. *Int. J. Climatol.* **33**, 121–131.

- Abatzoglou, J. T., R. Barbero, J. W. Wolf, and Z. A. Holden. 2014. Tracking interannual streamflow variability with drought indices in the US Pacific Northwest. *J. Hydrometeorol.* **15**, 1900–1912.
- Allen, C. D., A. K. Macalady, H. Chenchouni, D. Bachelet, N. McDowell, M. Vennetier, et al. 2010. A global overview of drought and heat-induced tree mortality reveals emerging climate change risks for forests. *For. Ecol. Manage.* **259**, 660–684.
- Alley, W. M. 1984. The palmer drought severity index: limitations and assumptions. *J. Climate Appl. Meteorol.* **23**, 1100–1109.
- Anderson, R. L., R. Byrne, and T. Dawson. 2008. Stable isotope evidence for a foggy climate on Santa Cruz Island, California At 16,600 Cal. Yr. BP. *Palaeogeogr. Palaeoclimatol. Palaeoecol.* **262**, 176–181.
- Assal, T. J., P. J. Anderson, and J. Sibold. 2016. Spatial and temporal trends of drought effects in a heterogeneous semi-arid forest ecosystem. *For. Ecol. Manage.* **365**, 137–151.
- Baguskas, S. A., S. H. Peterson, B. Bookhagen, and C. J. Still. 2014. Evaluating spatial patterns of drought-induced tree mortality in a Coastal California Pine Forest. *For. Ecol. Manage.* **315**, 43–53.
- Baguskas, S. A., C. J. Still, D. T. Fischer, C. M. D'Antonio, and J. Y. King. 2016. Coastal fog during summer drought improves the water status of sapling trees more than adult trees in a California Pine Forest. *Oecologia* **181**, 137–148.
- Barrett, B., C. Raab, and F. Cawkwell. 2016. Upland vegetation mapping using random forests with optical and radar satellite data. *Remote Sens. Ecol. Conserv.* **2**, 212–231.
- Boyle, T., and L. Laughrin. 2000. California's Santa Cruz Island weather. *Proceedings of the Fifth California Islands Symposium. US Department of the Interior, Minerals Management Service, Pacific OCS Region, Camarillo, California, USA*, 93–99.
- Brumbaugh, R. W. 1980. Recent geomorphic and vegetational dynamics on Santa Cruz Island, California. *The California Islands: Proceedings of a Multidisciplinary Symposium*. Pp. 139–158. Santa Barbara Museum of Natural History Santa Barbara, California, USA.
- Byer, S., and Y. Jin. 2017. Detecting drought-induced tree mortality in sierra Nevada forests with time series of satellite data. *Remote Sens.* **9**, 929.
- Carbone, M. S., C. J. Still, A. R. Ambrose, T. E. Dawson, A. Park Williams, C. M. Boot, et al. 2011. Seasonal and episodic moisture controls on plant and microbial contributions to soil respiration. *Oecologia* **167**, 265–278.
- Carbone, M. S., A. Park Williams, A. R. Ambrose, C. M. Boot, E. S. Bradley, T. E. Dawson, et al. 2013. Cloud shading and fog drip influence the metabolism of a coastal pine ecosystem. *Glob. Change Biol.* **19**, 484–497.
- Carlson, C. 2016. *Ventura County Trees Hard Hit by Drought, Infestations*. Ventura County Star. March 31, 2016. <http://archive.vcstar.com/news/special/outdoors/ventura-county-trees-hard-hit-by-drought-infestations-2ecfced6-ce17-031e-e053-0100007f182b-374157521.html>.
- Carnicer, J., M. Coll, M. Ninyerola, X. Pons, G. Sánchez, and J. Peñuelas. 2011. Widespread crown condition decline, food web disruption, and amplified tree mortality with increased climate change-type drought. *Proc. Natl Acad. Sci. USA* **108**, 1474–1478.
- Chaney, R. W., and H. L. Mason. 1930. *A Pleistocene Flora from Santa Cruz Island, California*. Vol. 415. Carnegie Institution, Washington, D.C.
- Choat, B., S. Jansen, T. J. Brodribb, H. Cochard, S. Delzon, R. Bhaskar, et al. 2012. Global convergence in the vulnerability of forests to drought. *Nature* **491**, 752–755.
- Cohen, B., C. Cory, J. Menke, and A. Hepburn. 2009. A spatial database of Santa Cruz Island vegetation. *Proceedings of the 7th California Islands Symposium. Institute for Wildlife Studies, Arcata, CA*, 229–244.
- Cohen, W. B., Z. Yang, and R. Kennedy. 2010. Detecting trends in forest disturbance and recovery using yearly Landsat time series: 2. Timesync — tools for calibration and validation. *Remote Sens. Environ.* **114**, 2911–2924.
- Cohen, W. B., S. P. Healey, Z. Yang, S. V. Stehman, C. Kenneth Brewer, E. B. Brooks, et al. 2017. How similar are forest disturbance maps derived from different Landsat time series algorithms? *For. Trees Livelihoods* **8**, 98.
- Deshayes, M., D. Guyon, H. Jeanjean, N. Stach, A. Jolly, and O. Hagolle. 2006. The contribution of remote sensing to the assessment of drought effects in forest ecosystems. *Ann. For. Sci.* **63**, 579–595.
- Diffenbaugh, N. S., D. L. Swain, and D. Touma. 2015. Anthropogenic warming has increased drought risk in California. *Proc. Natl Acad. Sci. USA* **112**, 3931–3936.
- Environmental Systems Research Institute (ESRI). 2018. *ArcMap Version 10.6*. Windows, Redlands, CA.
- Farjon, A. 2013. *Pinus muricata*. *The IUCN Red List of Threatened Species 2013*. e.T34058A2841776. International Union for Conservation of Nature, Gland.
- Fergusson, G. J., and W. F. Libby. 1963. UCLA radiocarbon dates II. *Radiocarbon* **5**, 1–22.
- Fischer, D. T., and C. J. Still. 2007. Evaluating patterns of fog water deposition and isotopic composition on the California Channel Islands. *Water Resour. Res.* **43**, 1135.
- Fischer, D. T., C. J. Still, and A. Park Williams. 2009. Significance of summer fog and overcast for drought stress and ecological functioning of coastal California endemic plant species. *J. Biogeogr.* **36**, 783–799.
- Fischer, D. T., C. J. Still, C. M. Ebert, S. A. Baguskas, and A. Park Williams. 2016. Fog drip maintains dry season ecological function in a California coastal pine forest. *Ecosphere* **7**, e01364.
- Foga, S., P. L. Scaramuzza, S. Guo, Z. Zhu, R. D. Dilley, T. Beckmann, et al. 2017. Cloud detection algorithm comparison and validation for operational Landsat data products. *Remote Sens. Environ.* **194**, 379–390.

- Forkel, M., N. Carvalhais, J. Verbesselt, M. D. Mahecha, C. S. R. Neigh, and M. Reichstein. 2013. Trend change detection in NDVI time series: effects of inter-annual variability and methodology. *Remote Sens.* **5**, 2113–2144.
- Fraser, R. H., I. Olthof, M. Carrière, A. Deschamps, and D. Pouliot. 2011. Detecting long-term changes to vegetation in Northern Canada using the Landsat satellite image archive. *Environ. Res. Lett.* **6**, 045502.
- Goodwin, N. R., N. C. Coops, M. A. Wulder, S. Gillanders, T. A. Schroeder, and T. Nelson. 2008. Estimation of insect infestation dynamics using a temporal sequence of Landsat data. *Remote Sens. Environ.* **112**, 3680–3689.
- Gorelick, N., M. Hancher, M. Dixon, S. Ilyushchenko, D. Thau, and R. Moore. 2017. Google earth engine: planetary-scale geospatial analysis for everyone. *Remote Sens. Environ.* **202**, 18–27.
- Huang, C., S. N. Goward, J. G. Masek, F. Gao, E. F. Vermote, N. Thomas, et al. 2009. Development of time series stacks of Landsat images for reconstructing forest disturbance history. *Int. J. Digital Earth* **2**, 195–218.
- Huang, C., S. N. Goward, J. G. Masek, N. Thomas, Z. Zhu, and J. E. Vogelmann. 2010. An automated approach for reconstructing recent forest disturbance history using dense Landsat time series stacks. *Remote Sens. Environ.* **114**, 183–198.
- Irons, J. R., J. L. Dwyer, and J. A. Barsi. 2012. The next Landsat satellite: the Landsat data continuity mission. *Remote Sens. Environ.* **122**(Suppl C), 11–21.
- Johnstone, J. A., and T. E. Dawson. 2010. Climatic context and ecological implications of summer fog decline in the coast redwood region. *Proc. Natl Acad. Sci. USA* **107**, 4533–4538.
- Jones, H. G., and R. A. Vaughan. 2010. *Remote Sensing of Vegetation: Principles, Techniques, and Applications*. Oxford University Press, Oxford, NY.
- Junak, S. 1995. *A Flora of Santa Cruz Island*. Santa Barbara Botanic Garden in collaboration with the California Native Plant Society, Santa Barbara, CA.
- Kennedy, R. E., Z. Yang, and W. B. Cohen. 2010. Detecting trends in forest disturbance and recovery using yearly Landsat time series: 1. LandTrendr—temporal segmentation algorithms. *Remote Sens. Environ.* **114**, 2897–2910.
- Kerr, J. T., and M. Ostrovsky. 2003. From space to species: ecological applications for remote sensing. *Trends Ecol. Evol.* **18**, 299–305.
- Key, C. H., and N. C. Benson. 2005. *The Normalized Burn Ratio (NBR): A Landsat TM Radiometric Measure of Burn Severity*, Report, US Geol. Surv, Boulder, CO Available at <http://nrmsc>.
- Kim, J. 2015. California's bishop pines are dying. Is drought to blame? Radio broadcast. *Morning Edition*. NPR. <https://www.npr.org/2015/06/02/411406467/californias-bishop-pines-are-dying-is-drought-to-blame>.
- Knapp, J. J., J. M. Randall, C. L. Boser, and S. A. Morrison. 2015. *Santa Cruz Island Ecological Management Strategy 2015–2025*. The Nature Conservancy, San Francisco, CA.
- Langin, K. M., T. Scott Sillett, W. Chris Funk, S. A. Morrison, M. A. Desrosiers, and C. K. Ghalambor. 2015. Islands within an Island: repeated adaptive divergence in a single population. *Evol. Int. J. Organ. Evol.* **69**, 653–665.
- Laughrin, L. 2017. *Letter to Annalise Taylor*. University of California Santa Barbara Natural Reserve System, Santa Cruz Island, CA.
- Liaw, A., and M. Wiener. 2002. Classification and regression by random forest. *R. News* **2**, 18–22.
- Lindenmayer, D. B., G. E. Likens, A. Andersen, D. Bowman, C. M. Bull, E. Burns, et al. 2012. Value of long-term ecological studies. *Austral Ecol.* **37**, 745–757. <https://doi.org/10.1111/j.1442-9993.2011.02351.x>.
- Little, E. L.; U. S. Geological Survey. 1999. Digital Representation of 'Atlas of United States Trees' by Elbert L. Little, Jr. US Geological Survey Professional Paper 1650, Lakewood, CO.
- Lloret, F., A. Lobo, H. Estevan, P. Maisongrande, J. Vayreda, and J. Terradas. 2007. Woody plant richness and NDVI response to drought events in Catalanian (northeastern Spain) forests. *Ecology* **88**, 2270–2279.
- Maselli, F. 2004. Monitoring forest conditions in a protected mediterranean coastal area by the analysis of multiyear NDVI data. *Remote Sens. Environ.* **89**, 423–433.
- McLaughlin, B. C., D. D. Ackerly, P. Zion Klos, J. Natali, T. E. Dawson, and S. E. Thompson. 2017. Hydrologic refugia, plants, and climate change. *Glob. Change Biol.* **23**, 2941–2961.
- Meddens, A. J. H., J. A. Hicke, L. A. Vierling, and A. T. Hudak. 2013. Evaluating methods to detect bark beetle-caused tree mortality using single-date and multi-date Landsat imagery. *Remote Sens. Environ.* **132**(Suppl C), 49–58.
- Morelli, T. L., C. Daly, S. Z. Dobrowski, D. M. Dulen, J. L. Ebersole, S. T. Jackson, et al. 2016. Managing climate change refugia for climate adaptation. *PLoS ONE* **11**, e0159909.
- Morrison, S. A., T. Scott Sillett, C. K. Ghalambor, J. W. Fitzpatrick, D. M. Graber, V. J. Bakker, et al. 2011. Proactive conservation management of an island-endemic bird species in the face of global change. *Bioscience* **61**, 1013–1021.
- Palumbo, I., R. A. Rose, R. M. K. Headley, J. Nackoney, A. Vodacek, and M. Wegmann. 2017. Building capacity in remote sensing for conservation: present and future challenges. *Remote Sens. Ecol. Conserv.* **3**, 21–29.
- Pasquarella, V. J., C. E. Holden, L. Kaufman, and C. E. Woodcock. 2016. From imagery to ecology: leveraging time series of all available Landsat observations to map and monitor ecosystem state and dynamics. *Remote Sens. Ecol. Conserv.* **2**, 152–170.
- Pesendorfer, M. B., T. Scott Sillett, and S. A. Morrison. 2017. Spatially biased dispersal of acorns by a scatter-hoarding corvid may accelerate passive restoration of oak habitat on California's largest island. *Curr. Zool.* **63**, 363–367.

- Powers, R. P., N. C. Coops, V. J. Tulloch, S. E. Gergel, T. A. Nelson, and M. A. Wulder. 2017. A conservation assessment of Canada's boreal forest incorporating alternate climate change scenarios. *Remote Sens. Ecol. Conserv.* **3**, 202–216.
- Rastogi, B., A. Park Williams, D. T. Fischer, S. F. Iacobellis, K. McEachern, L. Carvalho, et al. 2016. Spatial and temporal patterns of cloud cover and fog inundation in Coastal California: ecological implications. *Earth Interact.* **20**, 1–19.
- Robeson, S. M. 2015. Revisiting the recent California drought as an extreme value. *Geophys. Res. Lett.* **42**, 6771–6779.
- Robinson, N. P., B. W. Allred, M. O. Jones, A. Moreno, J. S. Kimball, D. E. Naugle, et al. 2017. A dynamic Landsat derived normalized difference vegetation index (NDVI) product for the conterminous United States. *Remote Sens.* **9**, 863.
- Robinson, N. P., B. W. Allred, W. K. Smith, M. O. Jones, A. Moreno, T. A. Erickson, et al. 2018. Terrestrial primary production for the conterminous United States derived from Landsat 30 m and MODIS 250 m. *Remote Sens. Ecol. Conserv.* **4**, 264–280.
- Rouse, J. W., Jr. 1974. *Monitoring the Vernal Advancement and Retrogradation (green Wave Effect) of Natural Vegetation*. <https://ntrs.nasa.gov/search.jsp?R=19740008955>.
- Schoenherr, A. A., C. Robert Feldmeth, and M. J. Emerson. 2003. *Natural History of the Islands of California*. University of California Press, Oakland, CA.
- Seager, R., M. Ting, I. Held, Y. Kushnir, L. Jian, G. Vecchi, et al. 2007. Model projections of an imminent transition to a more arid climate in Southwestern North America. *Science* **316**, 1181–1184.
- Stevens, M. 2016. 102 Million Dead California Trees 'Unprecedented in Our Modern History,' Officials Say. *Los Angeles Times*, November 18, 2016.
- Taylor, A. R. 2016. *Evaluating Spatial and Temporal Patterns of Bishop Pine (Pinus muricata) Mortality on Santa Cruz Island*. California, BA, Middlebury College.
- Verbesselt, J., R. Hyndman, G. Newnham, and D. Culvenor. 2010. Detecting trend and seasonal changes in satellite image time series. *Remote Sens. Environ.* **114**, 106–115.
- Vogelmann, J. E., G. Xian, C. Homer, and B. Tolk. 2012. Monitoring gradual ecosystem change using Landsat time series analyses: case studies in selected forest and rangeland ecosystems. *Remote Sens. Environ.* **122**, 92–105.
- Volcani, A., A. Karnieli, and T. Svoray. 2005. The use of remote sensing and GIS for spatio-temporal analysis of the physiological state of a semi-arid forest with respect to drought years. *For. Ecol. Manage.* **215**, 239–250.
- Walter, J. A., and R. V. Platt. 2013. Multi-temporal analysis reveals that predictors of mountain pine beetle infestation change during outbreak cycles. *For. Ecol. Manage.* **302**(Suppl C), 308–318.
- Walter, H. S., and L. A. Taha 1999. Regeneration of bishop pine (*Pinus muricata*) in the absence and presence of fire: a case study from Santa Cruz Island, California. *5th California Islands Symposium*. Pp. 172–181. Santa Barbara Museum of Natural History, Santa Barbara, CA.
- Wang, L., J. J. Qu, and X. Hao. 2008. Forest fire detection using the normalized multi-band drought index (NMDI) with satellite measurements. *Agric. For. Meteorol.* **148**, 1767–1776. <http://www.sciencedirect.com/science/article/pii/S0168192308001871>.
- Wehtje, W. 1994. Response of a bishop pine (*Pinus muricata*) population to removal of feral sheep on Santa Cruz Island, California. Pp. 331–340 in W. L. Halvorson and G. J. Maender, eds. *Update on the Status of Resources*. Santa Barbara Museum of Natural History, Santa Barbara, CA.
- Weiss, J. L., D. S. Gutzler, J. E. Allred Coonrod, and C. N. Dahm. 2004. Long-term vegetation monitoring with NDVI in a diverse semi-arid setting, central New Mexico, USA. *J. Arid Environ.* **58**, 249–272.
- Williams, A. P., C. J. Still, D. T. Fischer, and S. W. Leavitt. 2008. The influence of summertime fog and overcast clouds on the growth of a Coastal Californian Pine: A Tree-Ring Study. *Oecologia* **156**, 601–611.
- Wilson, E. H., and S. A. Sader. 2002. Detection of forest harvest type using multiple dates of Landsat TM imagery. *Remote Sens. Environ.* **80**, 385–396.
- Woodhouse, C. A., D. M. Meko, G. M. MacDonald, D. W. Stahle, and E. R. Cook. 2010. A 1,200-year perspective of 21st century drought in Southwestern North America. *Proc. Natl Acad. Sci. USA* **107**, 21283–21288.

## Supporting Information

Additional supporting information may be found online in the Supporting Information section at the end of the article.

**Appendix S1.** Supervised classifications of living vegetation, dead vegetation and open ground using a Random Forest classifier applied to two NAIP images captured on 5 May 2012 and 25 June 2016. Classification accuracy, as measured by an independent validation dataset, was 89.0% for the 2012 classification and 96.0% for the 2016 classification.

**Appendix S2.** Mean ( $\pm$ SE) per cent of area of grid cells ( $n = 1859$ ) classified as living vegetation, dead vegetation, and bare ground in NAIP image classifications from 2012 and 2016.

**Appendix S3.** Variable importance plot from the Random Forest regression using Landsat bands and derived vegetation indices to predict the percentage of living vegetation as quantified from NAIP imagery (Liaw and Wiener 2002).

**Appendix S4.** A zoomed-in view of a section of the bishop pine forest on Santa Cruz Island comparing the 1 m-pixel resolution 2012 NAIP image to a 29.86 cm-pixel resolution image of the same area in 2017 from the National Park Service. The inset map shows the location of this zoomed-in view on the island.